

# Experimental study on ultimate flexural capacity of steel encased concrete composite beams

Xiao Hui Li Aiqun Du Derun

(Key Laboratory of Concrete and Prestressed Concrete Structure of Ministry of Education, Southeast University, Nanjing 210096, China)

**Abstract:** Based on the experimental study and inelastic theory, the ultimate flexural capacity of steel encased concrete composite beams are derived. The difference between steel encased concrete composite beams with full shear connection and beams with partial shear connection, together with the relationship between the inelastic neutral axis of steel parts and concrete parts, are considered in the formulae. The calculation results of the eight specimens with full shear connection and the three specimens with partial shear connection are in good agreement with the experimental data, which validates the effectiveness and efficiency of the proposed calculation methods. Furthermore, the nonlinear finite element analysis of the ultimate flexural capacity of the steel encased concrete composite beams is performed. Nonlinear material properties and nonlinear contact properties are considered in the finite element analysis. The finite element analytical results also correlate well with the experimental data.

**Key words:** steel encased concrete composite beam; ultimate flexural capacity; finite element analysis

Steel encased concrete composite beams (see Fig. 1), a new type of composite beam, are formed by encasing concrete into the U-shaped groove welded by cold-formed profiled steel and a thick steel plane. The two parts of steel encased concrete composite beams cooperate with each other by the shear connectors such as the shear studs on the interfaces. The research results reveal that steel encased concrete composite beams have the advantages of improvement in flexural capacity, fire-resistance capacity and the comprehensive economic index of the beams, and convenience in construction process, compared with traditional composite beams<sup>[1]</sup>. According to the difference in the shear connection grade on the interfaces, steel encased concrete composite beams are divided into two kinds: beams with full shear connection and beams with partial shear connection<sup>[2]</sup>. If the total shear force in the shear connectors between the section with the maximum flexural moment and the minimum flexural moment is equal to the shear force calculated according to the ultimate equilibrium condition, the beams are beams with full shear connection. If not, the beams are ones with partial shear connection.

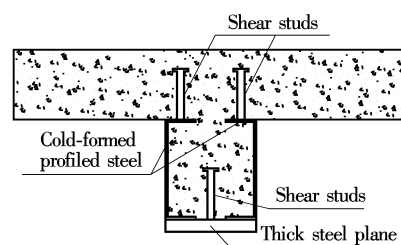


Fig. 1 Section of steel encased concrete composite beams

## 1 Experimental Study

In this study, eight specimens with full shear connection and three specimens with partial shear connection were tested to failure. All the specimens were simply supported and applied with vertical loads added step by step at the trisection points symmetrically. The strains in the steel and concrete were automatically collected by strain gauges connected in series by computer, and the deflection data were read from displacement gauges simultaneously.

Based on the crack patterns observed from the tested specimens, the failure modes of the steel encased concrete beams are classified into two types. One is the shear splitting failure mode which shows horizontal cracks along the interface between the steel flange and concrete or vertical cracks along the two longitudinal planes with all shear studs in the range of shear span; the other is the flexural failure mode which closely resembles the flexural failure of ordinary reinforced concrete beams. In this paper the methods for calculating the beams with the latter failure mode are investigated and proposed.

Fig. 2 shows the strains along the section of the specimen with full shear connection and those along the section of the specimen with partial shear connection respectively. It indicates that the steel encased concrete composite beams with full shear connection accord with the planar section assumption, but not the beams with partial shear

Received 2004-10-29.

**Foundation item:** The Code Program of Ministry of Construction of China.

**Biographies:** Xiao Hui (1980—), male, master; Li Aiqun (corresponding author), male, doctor, professor, aiqunli@sina.com.

connection due to the longitudinal slip effect on the interface between the two parts of the beams, as far as the whole composite section is concerned. In other words, the steel and the concrete in the beams with full shear connection have a uniform neutral axis; while the two parts of the beams with partial shear connection each has its own separate neutral axis. However, the research has proved that either part of the beams with partial shear connection can be separately assumed to accord with the planar section assumption.

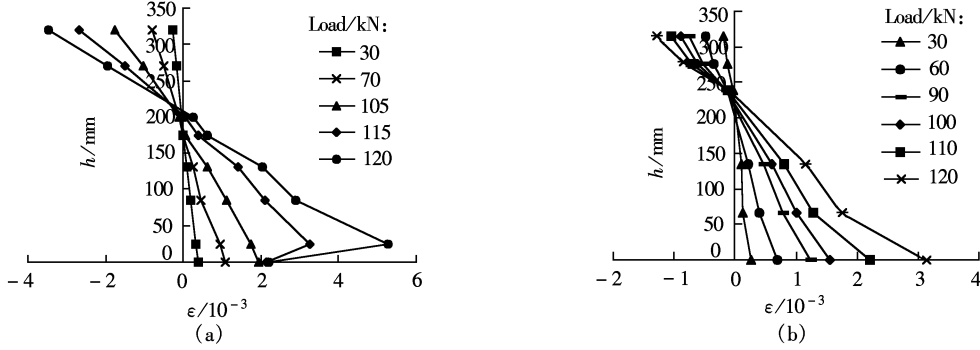


Fig. 2 Validation of planar section assumption. (a) Beams with full shear connection; (b) Beams with partial shear connection

## 2 Calculation Methods for Ultimate Flexural Capacity

The simply superposition method<sup>[3,4]</sup> and the universal superposition method<sup>[2,3]</sup> are in common use for calculating the ultimate flexural capacity of traditional steel-concrete composite beams. The former does not include the cooperation of the two parts of composite beams by considering them to work dividually and is adopted in the Japanese specification. Contrarily, the latter improves the deficiency of the former by considering the two parts to work together and is adopted in the most codes or specifications in the world. The universal superposition method is presented in this paper.

### 2.1 Steel encased concrete composite beams with full connection

The basic assumptions of the calculation for the ultimate flexural capacity of steel encased concrete composite beams include: ① The beam applied with load accords with the planar section assumption and the distribution of strains along the section is linear before the beam yields; ② The relationship between the strain and stress of steel, reinforced bars and concrete comes from the code for design of concrete structures of China (GB 50010 — 2002)<sup>[5]</sup>; ③ A uniformly distributed steel stress of  $0.9 f_y$ , the yielding stress of a steel section, is assumed throughout the tensile and compressive zones and the local bulking of a steel section is neglected; ④ A concrete stress of  $f_c$  is assumed to be uniformly distributed throughout the compressive zone, and the tensile strength of concrete is neglected; ⑤ The steel girder and concrete girder have the same curvatures.

According to different distributions of the plastic neutral axis (PNA) of the composite section, there are three classifications of calculations for the ultimate flexural capacity of steel encased concrete composite beams with full shear connection as follows.

#### 2.1.1 Plastic neutral axis within concrete flange

According to Fig. 3, the force and moment equilibriums give

$$f_c b_{cf} x - f_{ss} A_{ss} = 0 \quad (1)$$

$$M_u \leq 0.5 f_c b_{cf} x^2 + M_{tw} + M_{ts} \quad (2)$$

where  $M_{tw} = f_{tw} A_{tw} (h_0 - x)$ ;  $M_{ts} = f_{ts} A_{ts} (h - x - t_2/2)$ ;  $f_{ts}, f_{tw}$  are 0.9 times the yield strength of steel plane in the bottom and 0.9 times the yield strength of cold-formed profiled steel, respectively;  $A_{ts}$  is the area of the section of the steel plane in the bottom;  $A_{tw}$  is the area of the section of the cold-formed profiled steel;  $f_c$  is the concrete strength;  $M_u$  is the ultimate flexural capacity of the composite beams. In Fig. 3,  $x$  is the calculation depth of the compressive zone of concrete;  $x_0$  is the actual depth of the compressive zone of concrete,  $0.8x_0 = x$ ;  $h_{cf}$  is the height of the concrete flange;  $b_{cf}$  is the width of the concrete flange;  $b_{sf}$  is the width of the steel flange;  $h_s$  is the height of the steel girder;  $h$  is the height of the composite beam;  $b$  is the width of the web of the composite beam;  $t_1$  is the thickness of the cold-formed profiled steel;  $t_2$  is the thickness of the steel plane in the bottom;  $h_0$  is the distance between the centroid of cold-formed profiled steel and the surface of the concrete flange. From Eqs. (1) and (2), it can be seen that the plastic neutral axis is located in the concrete slab with a thickness of  $h_{cf}$  if  $0.8 f_c b_{cf} h_{cf} \geq f_{ss} A_{ss}$ , where  $f_{ss} A_{ss} = f_{ts} A_{ts} + f_{tw} A_{tw}$ , namely,  $x \leq h_{cf}$  and  $x_0 \leq h_{cf}$  in this case.

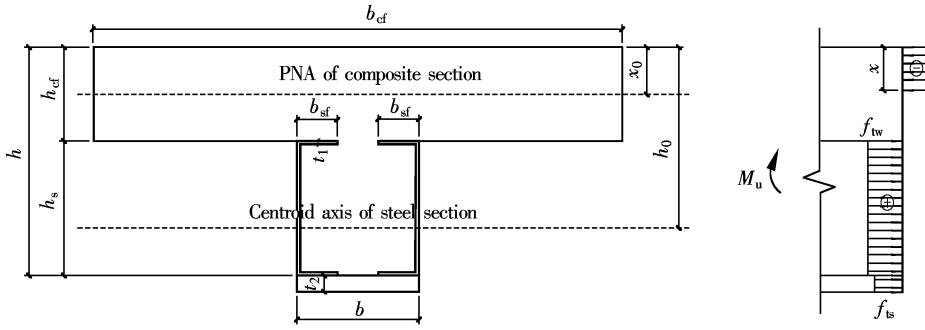


Fig. 3 Stress distribution when plastic neutral axis within concrete flange

### 2.1.2 Plastic neutral axis within steel flange

According to Fig. 4, the force and moment equilibriums give

$$f_c b_{cf} x + 4f_{tw} b_{sf} (1.25x - h_{cf}) - f_{ss} A_{ss} = 0 \quad (3)$$

$$M_u \leq 0.5f_c b_{cf} x^2 + M_{tw} + 2f_{tw} b_{sf} (1.25x - h_{cf}) (h_{cf} - 0.75x) + M_{ts} \quad (4)$$

Eqs. (3) and (4) indicate the condition that  $0.8f_c b_{cf} (h_{cf} + t_1) \geq f_{ss} A_{ss} \geq 0.8f_c b_{cf} h_{cf}$ , namely,  $x \leq h_{cf}$  and  $h_{cf} \leq x_0 \leq h_{cf} + t_1$  are satisfied.

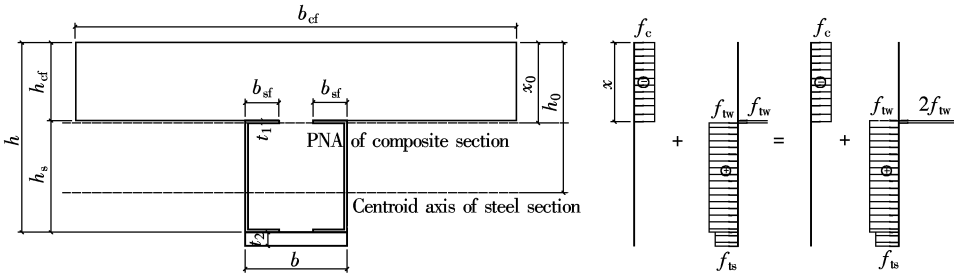


Fig. 4 Stress distribution when a plastic neutral axis is within steel flange

### 2.1.3 Plastic neutral axis in the web of a composite beam

Stress distribution when a plastic neutral axis is within the web of composite beam is shown in Fig. 5 and the categories are as follows:

- 1) If  $f_c b_{cf} h_{cf} \geq f_{ss} A_{ss} \geq 0.8f_c b_{cf} (h_{cf} + t_1)$ , namely,  $x \leq h_{cf}$  and  $x_0 \geq h_{cf} + t_1$ , the formulae can be expressed as

$$f_c b_{cf} x + 2f_{tw} [2b_{sf} t_1 + 2(1.25x - h_{cf} - t_1) t_1] - f_{ss} A_{ss} = 0 \quad (5)$$

$$M_u \leq 0.5f_c b_{cf} x^2 + M_{tw} + 4f_{tw} b_{sf} t_1 (h_{cf} + 0.5t_1 - x) + 2f_{tw} t_1 (1.25x - h_{cf} - t_1) (h_{cf} + t_1 - 0.75x) + M_{ts} \quad (6)$$

- 2) If  $f_c b_{cf} h_{cf} + f_c (b - 2b_{sf}) t_1 + 4f_{tw} t_1 b_{sf} \geq f_{ss} A_{ss}$ , namely,  $h_{cf} \leq x \leq h_{cf} + t_1$  and  $x_0 \geq h_{cf} + t_1$ , the formulae can be expressed as

$$f_c b_{cf} h_{cf} + f_c (b - 2b_{sf}) (x - h_{cf}) + 2f_{tw} [2b_{sf} t_1 + 2(1.25x - h_{cf} - t_1) t_1] - f_{ss} A_{ss} = 0 \quad (7)$$

$$M_u \leq f_c b_{cf} h_{cf} (x - 0.5h_{cf}) + M_{tw} + 4f_{tw} b_{sf} t_1 (h_{cf} + 0.5t_1 - x) + 2f_{tw} t_1 (1.25x - h_{cf} - t_1) (h_{cf} + t_1 - 0.75x) + M_{ts} \quad (8)$$

- 3) If  $f_c b_{cf} h_{cf} + f_c (b - 2b_{sf}) t_1 + 4f_{tw} t_1 b_{sf} \leq f_{ss} A_{ss}$ , namely,  $x \geq h_{cf} + t_1$  and  $x_0 \geq h_{cf} + t_1$ , the formulae can be expressed as

$$f_c b_{cf} h_{cf} + f_c (b - 2t_1) (x - h_{cf}) + 2f_{tw} [2b_{sf} t_1 + 2(1.25x - h_{cf} - t_1) t_1] - f_{ss} A_{ss} = 0 \quad (9)$$

$$M_u \leq f_c b_{cf} h_{cf} (x - 0.5h_{cf}) + 0.5f_c (b - 2t_1) (x - h_{cf})^2 + M_{tw} + 4f_{tw} b_{sf} t_1 (h_{cf} + 0.5t_1 - x) + 2f_{tw} t_1 (1.25x - h_{cf} - t_1) (h_{cf} + t_1 - 0.75x) + M_{ts} \quad (10)$$

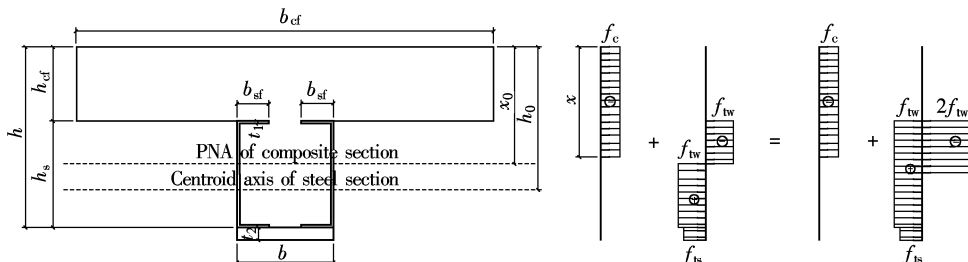


Fig. 5 Stress distribution when a plastic neutral axis is within the web of composite beam

In conclusion, the location of the plastic neutral axis and the depth of the concrete compression zone are estimated by  $x$  and  $1.25x$  on the assumption that the plastic neutral axis is firstly within the concrete flange, and then

the corresponding formulae are chosen for the calculation.

## 2.2 Steel encased concrete composite beams with partial shear connection

Steel encased concrete composite beams with large ratios of span to depth are popular in engineering design, where deflection is usually the key objective to be controlled. In fact, the shear studs of steel encased concrete composite beams with full shear connection do not yield or yield partly when the deflection of beams reaches the allowable limit in the service limit state design. Accordingly the composite beams are generally designed as ones with partial shear connection in engineering practices. Many engineering practices indicate that the adoption of beams with partial shear connection can reduce the amount of shear connectors used on the interfaces and increase the integrated economic benefits. As for beams with partial shear connection, the quantity, strength and distribution of shear connectors are the three dominating factors that affect the ultimate flexural capacity of beams. Furthermore, the shear connectors on all the interfaces including the flanges, webs and bottom plane of steel encased concrete beams contribute to the capacity, differently to traditional composite beams.

Based on the assumptions of calculation for steel encased concrete composite beams with full shear connection, the assumptions added for the ones with partial shear connection are established as follows: ① The steel and concrete in the beams accord with the planar section assumption of its own respectively; ② Shear connectors have sufficient transformation capacity; ③ The shear connectors are assumed to be ductile and work at the same load due to the plastic redistribution of the shear forces; ④ The bond between concrete and steel is neglected considering the lubricity of profiled steel beams.

The ultimate flexural capacity  $M_u$  is divided into two parts<sup>[2]</sup>:

$$M_u = M_s + Tz \quad (11)$$

where

$$T = \sum n_i V_{u,i} \quad (12)$$

$T$  is the total tensile stress needed to be added on the steel section when a steel beam is in the ultimate flexural state of itself;  $z$  is the distance between the centroid of the additional tensile stress and that of compressive stress of concrete;  $n_i$ ,  $V_{u,i}$  are the number and ultimate shear capacity of the  $i$ -th kind of shear connector, respectively;  $V_{u,i}$  refers to the code for design of concrete structures of China<sup>[5]</sup>. There are four classifications of calculations according to the position of a PNA of a steel beam and the edge line of a calculational expressive zone of a concrete beam.

### 2.2.1 Two axes within their own flanges

As shown in Fig. 6,

$$z = x_1 + h_{cf} - 0.5x \quad (13)$$

The force equilibriums give

$$T_1 - T_2 = T = \sum n_i V_{u,i} \quad (14)$$

$$T_1 + T_2 = A_{ss} f_{ss} \quad (15)$$

where  $x_1$  is the distance between the centroid of the additional tensile stress and the interfaces of the two parts of beams;  $T_1$  and  $T_2$  are the total stress in the tensile zone and that of the compressive zone of the steel beam, respectively.

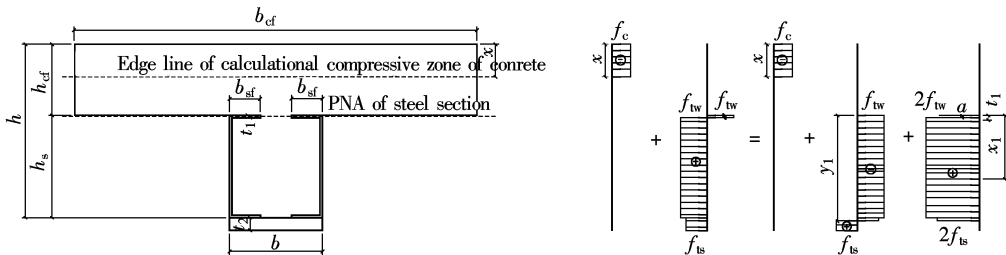


Fig. 6 Stress distribution when plastic neutral axes of steel beam and concrete beam are within their own flanges

Solving Eqs. (14) and (15) yields

$$T_1 = \frac{1}{2}(A_{ss} f_{ss} + \sum n_i V_{u,i}) \quad (16)$$

$$T_2 = \frac{1}{2}(A_{ss} f_{ss} - \sum n_i V_{u,i}) \quad (17)$$

So the depth of the compressive zone of the steel beam  $a$  is calculated by

$$a = \frac{T_2}{2f_{tw}b_{sf}} = \frac{A_{ss}f_{ss} - \sum n_i V_{u,i}}{4f_{tw}b_{sf}} \quad (18)$$

As shown in Fig. 6,

$$x_1 \approx a + \frac{1}{2}(y_1 - a) = \frac{1}{2}(y_1 + a) \quad (19)$$

where  $y_1$  is the distance between the centroid of the steel section and the top surface of the steel flange.

Derivating with respect to  $a$  in Eq. (18) and then using Eq. (19),

$$x_1 = \frac{1}{2} \left( y_1 + \frac{A_{ss}f_{ss} - \sum n_i V_{u,i}}{4f_{tw}b_{sf}} \right) \quad (20)$$

Derivating with respect to  $x_1$  in Eq. (20) and then using Eq. (16),

$$z = \frac{1}{2} \left( y_1 + \frac{A_{ss}f_{ss} - \sum n_i V_{u,i}}{4f_{tw}b_{sf}} \right) + h_{cf} - \frac{1}{2}x \quad (21)$$

### 2.2.2 Two axes within the steel web and the concrete flange respectively

From Fig. 7, the depth of the compressive zone of the steel beam  $a$  is calculated by

$$a = \frac{T_2 - 2f_{tw}b_{sf}h_{sf}}{2f_{tw}t_1} + t_1 = \frac{A_{ss}f_{ss} - \sum n_i V_{u,i}}{4f_{tw}t_1} - b_{sf} + t_1 \quad (22)$$

then

$$x_1 = \frac{1}{2} \left( y_1 + \frac{A_{ss}f_{ss} - \sum n_i V_{u,i}}{4f_{tw}b_{sf}} \right) - \frac{b_{sf} - t_1}{2} \quad (23)$$

$$z = \frac{1}{2} \left( y_1 + \frac{A_{ss}f_{ss} - \sum n_i V_{u,i}}{4f_{tw}b_{sf}} \right) - \frac{b_{sf} - t_1}{2} + h_{cf} - \frac{1}{2}x \quad (24)$$

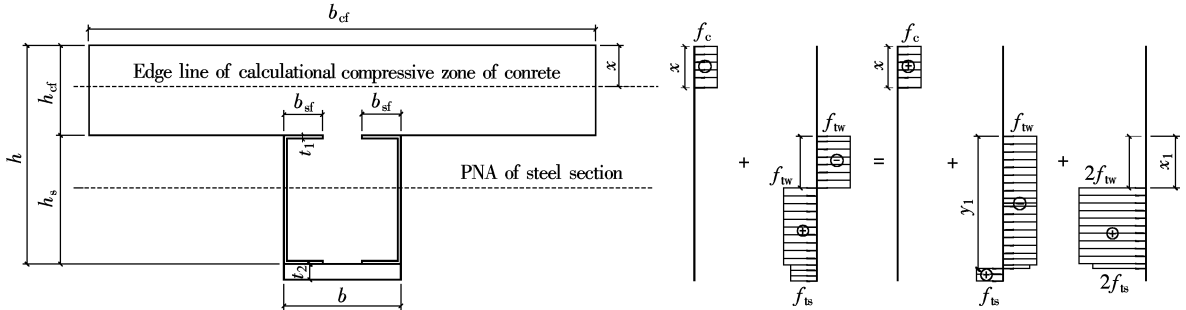


Fig. 7 Stress distribution when plastic neutral axes of steel beam and concrete beam are within a steel web and concrete flange

### 2.2.3 Two axes within concrete web and steel flange respectively

$$z = x_1 + h_{cf} - h_1 = z = \frac{1}{2} \left( y_1 + \frac{A_{ss}f_{ss} - \sum n_i V_{u,i}}{4f_{tw}b_{sf}} \right) + h_{cf} - h_1 \quad (25)$$

where  $h_1$  is the distance between the centroid of the compressive zone of concrete beams and the top surface of composite beams.

### 2.2.4 Two axes within their own webs

$$z = \frac{1}{2} \left( y_1 + \frac{A_{ss}f_{ss} - \sum n_i V_{u,i}}{4f_{tw}b_{sf}} \right) - \frac{b_{sf} - t_1}{2} + h_{cf} - h_1 \quad (26)$$

Based on Eqs. (21), (24), (25) and (26), solving Eq. (11) yields the ultimate flexural capacity of steel encased concrete beams with partial shear connection.

## 3 Nonlinear Finite Element Analysis of Ultimate Flexural Capacity

Nonlinear finite element analysis, a practical way of parametric studies on the characteristics of steel encased concrete composite beams, is performed by means of the software ANSYS 6.1. In the analysis, the concrete is simulated as element Solid65, and the relationship between the stress and strain of concrete adopts the multilinear kinematics hardening plasticity model. The failure state of the compressive zone accords with the Willam-Warnke failure criterion, which depends on five material parameters. The relationship between the stress and strain of cold-formed profiled steel is accomplished by the definition of bilinear kinematics hardening plasticity. In addition, every shear

connector is modeled as three spring elements. Among the three spring elements, the transverse and vertical elements are Combin14 with high rigidity; while the longitudinal element adopts Combin39, a nonlinear element to simulate the nonlinear properties of a shear connector. Based on Ref. [6], the equation  $V = V_u (1 - e^{-0.702s})^{0.4}$  gives the relationship between the shear force and relative slip of Combin39, where  $V_u$  is concerned before. Furthermore, the point-to-point contact is used to simulate the contact between the two parts of beams and the friction rigidity is defined as zero for simple consideration.

4 Results

As shown in Tab. 1, the results of calculation and finite element analysis correlate well with the experimental data, which validates the effectiveness and efficiency of the proposed calculation methods and the nonlinear finite element analysis.  $M_u^c$ ,  $M_u^f$  and  $M_u^t$  represent the results of calculation, finite element analysis and experiment, respectively. Specimen 1 to specimen 3 are beams with partial connection and the others are ones with full connection.

Tab. 1 Comparison among the results of experiment, calculation and finite element analysis

| Specimen | $h_{st}/mm$ | $b_{st}/mm$ | $b_{st}/mm$ | $b/mm$ | $t_f/mm$ | $t_w/mm$ | $h/mm$ | $L/mm$ | $M_u^c /$<br>(kN·m) | $M_u^f /$<br>(kN·m) | $M_u^t /$<br>(kN·m) | $M_u^c / M_u^t$ | $M_u^f / M_u^t$ |
|----------|-------------|-------------|-------------|--------|----------|----------|--------|--------|---------------------|---------------------|---------------------|-----------------|-----------------|
| 1        | 115         | 900         | 50          | 150    | 4        | 20       | 360    | 6.45   | 346                 | 310                 | 376                 | 0.918           | 0.824           |
| 2        | 110         | 900         | 50          | 150    | 4        | 20       | 360    | 6.45   | 409                 | 359                 | 440                 | 0.929           | 0.815           |
| 3        | 110         | 900         | 50          | 300    | 4        | 20       | 220    | 5.25   | 352                 | 304                 | 366                 | 0.962           | 0.831           |
| 4        | 110         | 900         | 50          | 300    | 4        | 20       | 220    | 5.25   | 352                 | 294                 | 355                 | 0.991           | 0.828           |
| 5        | 115         | 1 500       | 50          | 340    | 4        | 14       | 315    | 6.60   | 551                 | 459                 | 550                 | 1.002           | 0.834           |
| 6        | 115         | 1 500       | 50          | 340    | 4        | 14       | 315    | 6.60   | 550                 | 464                 | 561                 | 0.980           | 0.827           |
| 7        | 120         | 1 100       | 50          | 290    | 4        | 14       | 360    | 6.60   | 559                 | 459                 | 561                 | 0.996           | 0.818           |
| 8        | 120         | 1 100       | 50          | 290    | 4        | 14       | 360    | 6.60   | 557                 | 470                 | 572                 | 0.974           | 0.822           |
| 9        | 100         | 890         | 50          | 180    | 4        | 20       | 345    | 6.45   | 234                 | 203                 | 255                 | 0.917           | 0.795           |
| 10       | 115         | 900         | 50          | 180    | 4        | 20       | 360    | 6.45   | 280                 | 230                 | 287                 | 0.974           | 0.802           |
| 11       | 115         | 890         | 50          | 180    | 4        | 20       | 360    | 6.45   | 331                 | 292                 | 372                 | 0.890           | 0.786           |

References

[1] Zhao Hongtie. *Composite steel-concrete structure* [M]. Beijing: Science Press, 2001. 1 – 4. (in Chinese)

[2] Nie Jianguo, Cui Yuping, Shi Zhongzhu, et al. Ultimate flexural capacity of composite steel-concrete beams with partial shear connection [J]. *Engineering Mechanics*, 2000, **17**(3): 37 – 42. (in Chinese)

[3] Wang Ting, Nie Jianguo, Li Bingyi, et al. Study on ultimate flexural capacity of composite steel-concrete beams with profiled sheeting [J]. *Journal of Building Structures*, 2001, **22**(2): 61 – 65. (in Chinese)

[4] Commission of European Norm. Eurocode No. 4 — 1992 Design of composite steel and concrete structures[S]. London: British Standards Institution, 1992.

[5] Ministry of Construction of China. GB 50010 — 2002 Code for design of concrete structures [S]. Beijing: China Architecture & Building Press, 2002. (in Chinese)

[6] Lu Xinzheng, Jiang Jianjing. Analysis of complicated stress of concrete composite component with Solid65, a kind of element of ANSYS [J]. *Building Structure*, 2003, **33**(6): 22 – 24. (in Chinese)

外包钢-混凝土组合梁正截面极限抗弯承载力的试验研究

肖 辉 李爱群 杜德润

(东南大学混凝土与预应力混凝土结构教育部重点实验室, 南京 210096)

摘要: 基于外包钢-混凝土组合梁的试验研究和塑性理论, 按照钢梁和混凝土塑性中和轴相对位置的不同, 分别推导了完全剪切连接和部分剪切连接的外包钢-混凝土组合梁的正截面极限抗弯承载力的计算公式, 对外包钢-混凝土组合梁进行了非线性有限元分析, 分析中重点考虑了材料非线性和接触非线性. 8 根完全剪切连接和 3 根部分剪切连接试件的正截面极限抗弯承载力的计算结果及有限元分析结果与试验结果吻合良好.

关键词: 外包钢-混凝土组合梁; 极限抗弯承载力; 有限元分析

中图分类号: TU378. 2